ELSEVIER

Physica A 207 (1994) 334–339

PHYSICA A

Optical reflectance anisotropy of Ag and Au (110) single crystals

W.L. Mochán[a], R.G. Barrera[b], Y. Borensztein[c], A. Tadjeddine[d]

[a]*Laboratorio de Cuernavaca, Instituto de Fisica, UNAM, Apartado Postal 139-B, 62191 Cuernavaca, Morelos, Mexico*

[b]*Instituto de Fisica, UNAM, Apartado Postal 20-364, 01000 Mexico D.F., Mexico*

[c]*Laboratoire d'Optique des Solides, UA CNRS 781, Université P. et M. Curie, 4 place Jussieu, 75252 Paris Cedex 05, France*

[d]*Laboratoire d'Electrochimie de Interfaces, CNRS, 1 pl. Aristide Briand, 92195 Meudon Cedex, France*

Abstract

We have developed a theoretical model for describing the electromagnetic response of noble metal surfaces. The model takes into account the d to s–p interband transitions as well the actual crystalline geometry. The surface response is incorporated in a calculation of the optical reflectance, and it yields corrections to Fresnel's formulae which depend on the angle between the polarization vector and the surface principal directions. The anisotropy effect has been confirmed by surface reflectance anisotropy spectroscopy experiments performed on (110) Ag and Au surfaces. We show that the main contribution to the anisotropy is the screened surface local-field effect on resonant dipolar oscillations localized near the surface.

1. Introduction

Since the linear, long-wavelength, bulk electromagnetic response of a cubic crystal is isotropic, any anisotropies in its optical properties are expected to originate from the lower symmetry of its surface. The measurement of the reflection anisotropy of cubic crystals has become an important tool for the investigation of surface structure [1–5]. There are many possible sources of anisotropy, such as transitions among surface states [6,7] and preferential surface roughness, though intrinsic anisotropies at flat surfaces in the absence of surface states have also been observed [1]. These anisotropies have been successfully accounted for in some systems by the surface local-field effect [8].

Lately, there has been a renewed interest in the electromagnetic response of single crystal Ag surfaces. After the pioneering research of Furtak and Lynch [9]

SSDI 0378-4371(93)E0574-X

who showed an anisotropy in the electroreflectance spectra of Ag (110), came the work of Tadjeddine et al. [10] who measured attenuated total reflection spectra and found that the dispersion relation of the retarded surface plasmons on Ag surfaces depended on the face orientation and on their propagation direction. The nonretarded surface plasmon dispersion has recently been measured [11–13] by electron energy-loss spectroscopy, and an anomalous anisotropic dispersion whose kind is still in dispute [14–16] was also found.

The bulk and surface plasmons of Ag have frequencies that are substantially lower than what might be expected in terms of the free electron theory [17]. This is due to a large positive contribution to the real part of the dielectric function originated from the interband transitions between a d-band complex below the Fermi energy and the conduction s–p band [18]. In this paper we extend a model previously employed to incorporate the surface geometry and the contributions of both, interband and intraband, transitions in a calculation of the collective modes of Ag surfaces [19]. Here we calculate the surface optical conductivity and employ it to obtain the surface corrections to the complex reflection amplitude. We apply the model to Ag and Au (110) surfaces and we obtain that their reflection amplitude is anisotropic. The reflectance anisotropy (RA) spectra of Au turn out to be of the same order of magnitude as that of previously investigated systems, but that of Ag is about two orders of magnitude larger. To test this result we performed RA measurements and compared them to the theoretical results.

2. Model

Following ref. [19], we assume that, since the d orbitals are fairly localized, the interband transitions generate dipole moments only in small regions localized near the ionic core positions where there is a substantial overlap between the d and the s–p wavefunctions. Furthermore, we assume that outside these regions the conduction electron gas can be assumed to be homogeneous. Therefore, we model the crystal as an homogeneous electron gas with a *swiss cheese* geometry, with spherical cavities centered at every fcc lattice site. We replace the ionic core, the d electrons and the electron gas within each sphere by a point polarizable entity located at the center of the cavity. We describe the electron gas by the simple Drude model and we characterize each dipole by its polarizability, which is fixed by the requirement that the calculated bulk macroscopic dielectric response should agree with experiment.

The total dipole moment $\boldsymbol{p}_i$ within the ith cavity is given by

$$\boldsymbol{p}_i = \alpha\left(\boldsymbol{E}_0 + \sum_{j\neq i} T_{ij}\boldsymbol{p}_j + \sum_{j'} T_{ij'}\boldsymbol{p}_{j'}\right), \qquad \boldsymbol{E}_0 = \left(E^x, E^y, \frac{E^z}{\varepsilon_g}\right),$$

$$\varepsilon_g = 1 - \frac{\omega_g^2}{(\omega^2 + i\omega\tau)}, \tag{1}$$

where $\boldsymbol{E}_0$ is the external field, whose component normal to the surface E^z is screened by the dielectric response ε_g of the conduction electron gas, $T_{ij}=\nabla\nabla R_{ij}^{-1}$ is the bare dipole–dipole interaction, and $\boldsymbol{p}_{j'}$ is the image of the dipole $\boldsymbol{p}_j$, reflected from inside by the boundary of the electron gas.

For a long-wavelength field, all the dipoles acquire essentially the same moment within the bulk $\boldsymbol{p}_j=\boldsymbol{p}_B$, so that Eq. (1) is very simply solved, yielding the well known Clausius–Mossotti relation [20] $(\varepsilon-\varepsilon_g)/(\varepsilon+2\varepsilon_g)=\frac{4}{3}\pi n\alpha$, where n is the number density. Now we set ε to the experimentally measured [17] bulk dielectric function $\varepsilon_{ex}(\omega)$ for each frequency ω, we solve the previous equation for the bulk polarizability α, we assume that α is independent of position and solve Eq. (1) to obtain $\boldsymbol{p}_i$ in the neighborhood of the surface [21].

Under normal incidence, the electromagnetic response of the surface may be characterized by the surface conductivity [22] σ defined through $\boldsymbol{i}_{\parallel}\equiv\sigma\boldsymbol{E}_{\parallel}(0)$, where $\boldsymbol{i}=\int \mathrm{d}^3r\,(\boldsymbol{j}-\boldsymbol{j}_B)/A$ measures the difference between the electric current density $\boldsymbol{j}$ near the surface and its bulk value $\boldsymbol{j}_B$, and A is the area of the sample. Taking account that both the localized dipoles and the electron gas contribute to $\boldsymbol{j}$, it can be shown [8,9,21] that

$$\sigma=-\mathrm{i}\omega a\,\frac{\varepsilon-\varepsilon_g}{4\pi}\sum_n\frac{(p_n)_{\parallel}-(p_B)_{\parallel}}{(p_B)_{\parallel}}, \tag{2}$$

where the sum is taken over the crystalline planes n.

Finally, the normal incidence complex reflection amplitude is given by [8,22]

$$r=r_f\left(1+\frac{8\pi\sigma/c}{\varepsilon-1}\right), \qquad r_f=(\sqrt{\varepsilon}-1)/(\sqrt{\varepsilon}+1) \tag{3}$$

where r_f is the Fresnel reflectance.

3. Results

In Fig. 1 we show the surface conductivities σ of the (110) face of Au and Ag crystals for the electric field along the two nonequivalent principal directions $[1\bar{1}0]$ and [001]. Notice that there is a resonant structure that corresponds to dipolar surface excitations, and that the surface conductivity displays a very marked anisotropy. We observe very wide peaks in the conductivities of Au and better defined ones for Ag, particularly for the [001] orientation. This structure may be understood in terms of the resonances of α shifted in frequency by the dipole–dipole and by the dipole–image interactions; it corresponds to normal oscillations of the dipole moments localized within the first few atomic planes. In the case of Ag(110)[001] the peak lies very close to the surface-plasmon frequency and below the interband threshold where dissipation is very small, so it is much larger and narrower than the others.

Using the above conductivities we have calculated the real and imaginary parts

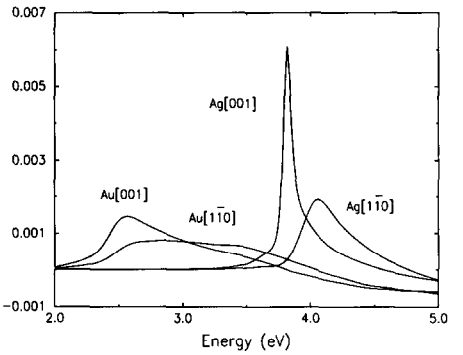

Fig. 1. Real part of the surface conductivity of Ag and Au (110) surfaces for fields along [1$\bar{1}$0] and [001].

of the reflection amplitudes r for $\boldsymbol{E}$ along [1$\bar{1}$0] and [001], and the relative RA $\Delta r/r = (r_{[1\bar{1}0]} - r_{[001]})/r_{[001]}$. We have also performed measurements of the RA using what can be considered a normal incidence ellipsometer developed by the ISA Jobin–Yvon company (France). The RA signal may be obtained from the ellipsometric parameters ψ and Δ defined through $r_{[001]}/r_{[1\bar{1}0]} = \tan\Psi\, e^{i\Delta}$. The apparatus [23] consists of a 75 W xenon lamp as a source of light that hits the sample at 2.75°. The light is polarized and analyzed with Glan–Taylor polarizers and modulated with a fused silica bar subject to a 50 kHz periodical stress. Its energy is analyzed with a double-grating monochromator and detected with a photomultiplier with a range 230–830 nm. The sample was prepared following a procedure [24] which produces well defined single-crystal surfaces.

In Fig. 2 we display the real part of the reflectance anisotropy $\Delta r/r$ of Au (110).

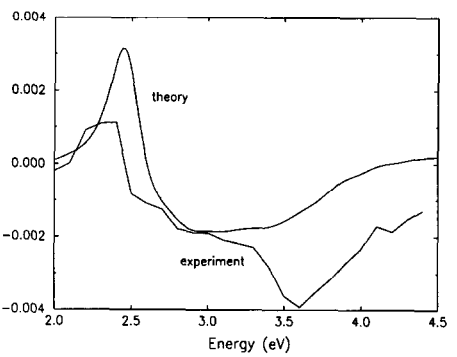

Fig. 2.

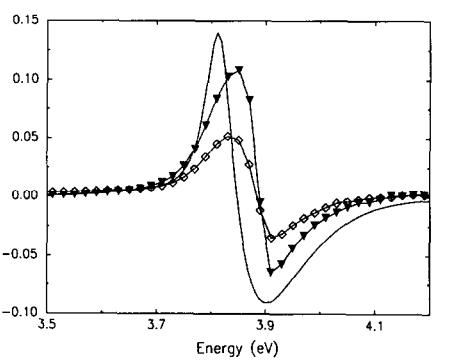

Fig. 3.

Fig. 2. Real part of the calculated and measured reflectance anisotropy spectra (Re ($\Delta r/r$)) of a Au (110) surface.

Fig. 3. Real part of the calculated and measured reflectance anisotropy spectra (Re($\Delta r/r$)) of a Ag (110) surface. The open diamonds and closed triangles correspond to the freshly prepared and the 48 h old samples.

Both theory and experiment show an anisotropy of the same order of magnitude as previously obtained for semiconductors, i.e., a few parts in a thousand. The calculated results agree roughly with experiment: they are of the same order of magnitude, they follow the same pattern of sign reversals and they have the same peak-to-peak amplitude. However, the experiment shows a distinct structure at 3.6 eV that is absent in the calculated results.

In Fig. 3 we show the real part of the RA calculated for Ag and experimental results for two samples, one prepared just prior to the measurement and the other prepared 48 h in advance and stored in an air ambient. In this case the theoretical and the experimental results are both two orders of magnitude larger than for Au and for other systems [1]. One reason for this anisotropy enhancement is the large resonance in the surface conductivity of Ag. Another reason is the sharp decrease in the reflectivity r of Ag at the plasma frequency, which enhances the relative anisotropy $\Delta r/r$. The three have a high degree of correspondence and there is a good quantitative agreement between the measurements on the oxidized crystal and theory. This might be due to an overestimation of the surface local field effect by our point dipole model together with an overlayer induced decrease in r for the contaminated sample.

4. Conclusions

We developed a model with which we calculated the reflectance anisotropy of Ag and Au (110) surfaces incorporating the conduction electron gas, the interband transitions and the crystalline geometry. We also performed normal-incidence ellipsometry experiments to measure the RA signal. For Au we obtained a qualitative agreement between theory and experiment. For Ag the theory yields an extremely large optical anisotropy which is in very good accord with experiment. Several causes of anisotropy might be present, such as an anisotropic electron gas conductivity or presence of anisotropic film coatings. However, our results show that the local-field effect plays a most important role in the surface optical response of the noble metals. They also confirm that optical anisotropy spectroscopy is a linear optical technique that is inherently sensitive to the surface and that may be employed in environments in which other surface techniques are ineffective.

Acknowledgements

RGB and WLM acknowledge the partial support of DGAPA-UNAM under Contract No. IN-102493.

References

[1] D.E. Aspnes and A.A. Studna, Phys. Rev. Lett. 54 (1985) 1956.
[2] S. Selci, F. Ciccacci, A. Cricenti, A.C. Felici, C. Goletti and P. Chiaradia, Solid State Commun. 62 (1987) 833.
[3] D.E. Aspnes et al., Phys. Rev. Lett. 61 (1988) 2782.
[4] S.E. Acosta-Ortiz and A. Lastras-Martínez, Phys. Rev. B 40 (1989) 1426.
[5] S.M. Koch et al., J. Appl. Phys. 69 (1991) 1389.
[6] K.M. Ho, B.N. Harmon, and S.H. Liu, Phys. Rev. Lett. 44 (1980) 1531.
[7] M.Y. Jiang, G. Pajer and E. Burstein, Surf. Sci. 242 (1991) 306.
[8] W. Luis Mochán and Rubén G. Barrera, Phys. Rev. Lett. 55 (1985) 1192.
[9] T.E. Furtak and D.W. Lynch, Phys. Rev. Lett. 35 (1975) 960.
[10] A. Tadjeddine, D.M. Kolb and R. Kötz, Surf. Sci. 101 (1980) 277.
[11] R. Contini and J.M. Layet, Solid State Commun. 64 (1987) 1179.
[12] M. Rocca and U. Valbusa, Phys. Rev. Lett. 64 (1992) 2398.
[13] M. Rocca, M. Lazzarino and U. Valbusa, Phys. Rev. Lett. 69 (1992) 2122.
[14] S. Suto, K.D. Tsuei, E.W. Plummer and E. Burstein, Phys. Rev. Lett. 63 (1989) 2590.
[15] M. Rocca, M. Lazzarino and U. Valbusa, Phys. Rev. Lett. 67 (1991) 3197.
[16] G. Lee, P.T. Sprunger, E.W. Plummer and S. Suto Phys. Rev. Lett. 67 (1991) 3198.
[17] P.B. Johnson and R.W. Christy, Phys. Rev. B 6 (1972) 4370.
[18] G. Fuster et al., Phys. Rev. B 42 (1990) 7322.
[19] Jesús Tarriba and W. Luis Mochán, Phys. Rev. B 46 (1992) 12902.
[20] E. Fiorino and R. Del Sole, Phys. Status Solidi B 119 (1983) 315.
[21] W.L. Mochán and R.G. Barrera, J. Phys. Colloq. 45 (1984) C5-207.
[22] W. Luis Mochán, Ronald Fuchs and R.G. Barrera, Phys. Rev. B 27 (1983) 771.
[23] O. Acher and B. Drevillon, Rev. Sci. Instrum. 63 (1992) 5332.
[24] A. Hamelin, L. Stoicoviciu, L. Dubova and S. Trasatti, Surf. Sci. 201 (1988) L496.